ELSEVIER

Biochimica et Biophysica Acta 1421 (1999) 329–339

BIOCHIMICA ET BIOPHYSICA ACTA
BBA

www.elsevier.com/locate/bba

Localization of sterically stabilized liposomes in *Klebsiella pneumoniae*-infected rat lung tissue: influence of liposome characteristics

Raymond M. Schiffelers [a,b,*], Irma A.J.M. Bakker-Woudenberg [b], Susan V. Snijders [b], Gert Storm [a]

[a] *Department of Pharmaceutics, Utrecht Institute for Pharmaceutical Sciences (UIPS), Utrecht University, P.O. Box 80082, 3508 TB Utrecht, The Netherlands*

[b] *Department of Medical Microbiology and Infectious Diseases, Erasmus University Medical Center Rotterdam (EMCR), P.O. Box 1738, 3000 DR Rotterdam, The Netherlands*

Received 12 July 1999; received in revised form 6 August 1999; accepted 12 August 1999

Abstract

Sterically stabilized liposomes are able to localize at sites of infection and could serve as carriers of antimicrobial agents. For a rational optimization of liposome localization, the blood clearance kinetics and biodistribution of liposomes differing in poly(ethylene glycol) (PEG) density, particle size, bilayer fluidity or surface charge were studied in a rat model of a unilateral pneumonia caused by *Klebsiella pneumoniae*. It is shown that all liposome preparations studied localize preferentially in the infected lung compared to the contralateral non-infected lung. A reduction of the PEG density or rise in particle size resulted in a higher uptake by the mononuclear phagocyte system, lower blood circulation time and lower infected lung localization. Differences in bilayer fluidity did not affect blood clearance kinetics or localization in the infected lung. Increasing the amount of negatively charged phospholipids in the liposome bilayer did not affect blood clearance kinetics, but did reduce localization of this liposome preparation at the site of lung infection. In conclusion, the degree of localization at the infected site is remarkably independent of the physicochemical characteristics of the PEG liposomes. Substantial selective liposome localization can be achieved provided that certain criteria regarding PEG density, size and inclusion of charged phospholipids are met. These properties seem to be a direct consequence of the presence of the polymer coating operating as a repulsive steric barrier opposing interactions with biological components.

Keywords: Sterically stabilized liposome; Poly(ethylene glycol); Pharmacokinetics; Pneumonia; Rat; Targeting; Infection

1. Introduction

Unfavorable location of an infectious organism, limited susceptibility to the applied antimicrobial agent and/or a decreased immune status of the infected host are all major factors complicating the efficacy of antimicrobial therapy [1–3]. The use of a drug carrier, like liposomes, could help to improve

* Corresponding author. Fax: +31 (10) 4089454; E-mail: schiffelers@kmic.fgg.eur.nl

0005-2736/99/$ – see front matter
PII: S0005-2736(99)00139-X

the efficacy of antibiotic treatment by modifying the pharmacokinetics and tissue distribution of the antibiotic. This strategy may increase drug concentrations at the target site and/or reduce toxicity to non-target tissues enabling higher dosing [4,5].

The location of the infection is an important consideration for the choice of the liposome type to be used as targeted antibiotic carrier. As intravenously administered conventional liposomes display a high affinity for the mononuclear phagocyte system (MPS), a rapid localization of these liposomes in MPS-rich organs, most notably in the liver and the spleen, is observed. This property makes them appropriate for the specific targeting of antimicrobials to infectious organisms residing within MPS cells in these organs. In addition, since the MPS plays an important role in the non-specific defense against infections, MPS-directed targeting of liposomal immunomodulators may enhance the non-specific host resistance. Both strategies have been reviewed [6,7].

The limitations of these conventional liposomes as antibiotic carriers are clear when targeting to infections outside the MPS is the main goal. Various strategies have been followed to reduce uptake of liposomes by the MPS and consequently to increase their blood residence time, allowing for interaction with other tissues. At present, coating of the surface of liposomes with poly(ethylene glycol) (PEG) is a popular strategy to increase the circulation time of liposomes. It is thought that the PEG coating provides a steric barrier against opsonization, thereby reducing the interaction with the MPS. Consequently, these liposomes, referred to as sterically stabilized liposomes (SSL), exhibit a prolonged circulation time (for reviews see [8–10]).

Previous studies of our group in a model of acute unilateral pneumonia caused by *Klebsiella pneumoniae* in rats demonstrated that SSL are capable to substantially localize in the infected left lung. The presence of a local active infectious process appeared to be required as minimal liposome localization was observed in the contralateral non-infected right lung [11,12]. Furthermore, it was shown that encapsulated gentamicin was strongly effective in reducing bacterial numbers in the infected left lung as well as preventing mortality, likely due to local release of the drug from the SSL at the site of infection [13].

The phenomenon of preferential localization of SSL at pathological sites has also been described for other inflammatory conditions like adjuvant arthritis in rats, experimental colitis in rabbits, focal bacterial infection in the calf muscle of rats and osteomyelitis in rabbits [14–17]. However, only little information is available on the influence of liposome characteristics on the degree of localization of SSL at inflammatory foci. Insight into the liposomal properties favoring the localization in inflammatory tissue may help to optimize liposomal formulations for antimicrobial therapy. The aim of the present study is to evaluate the effects of PEG surface density, particle size, bilayer fluidity and surface charge of SSL on circulation kinetics and localization in infected lung tissue.

2. Materials and methods

2.1. Introduction of a unilateral pneumonia

Specified pathogen-free female RP/AEur/RijHsd strain albino rats (18–25 weeks of age, weighing 185–225 g) (Harlan, Horst, The Netherlands) were used in all experiments. Experiments were approved by the animal experiments ethical committee of the Erasmus University Medical Center Rotterdam. A unilateral pneumonia was induced in the left lung as described previously [18]. In brief, rats were anesthetized by an intramuscular injection of 0.1 ml fluanisone and fentanyl citrate (Hypnorm) (Janssen Animal Health, Saunderton, UK) followed by an intraperitoneal injection of 0.3 ml 1:4 v/v diluted pentobarbital (Nembutal) (Sanofi Santé, Maassluis, The Netherlands). After incubation followed by cannulation of the left primary bronchus, 0.02 ml of a saline suspension containing 10^6 *K. pneumoniae* (ATCC 43816, capsular serotype 2) was inoculated in the lower left lung lobe. Bacterial inoculum was checked by culturing appropriate dilutions of the bacterial suspension on tryptone soy agar plates (Unipath, Basingstoke, UK). Following bacterial inoculation, rats received an intramuscular injection of nalorphine bromide to recover from anesthesia (Onderlinge Pharmaceutische Groothandel, Utrecht, The Netherlands) and were housed individually with free access to water and SRMA chow (Hope Farms, Woerden, The Netherlands).

2.2. Liposome preparation and characterization

Liposomes were prepared as described previously [12]. In brief, appropriate amounts of partially hydrogenated egg phosphatidylcholine (PHEPC, iodination value 40) (Asahi Chemical Industry, Ibarakiken, Japan), cholesterol (Chol) (Sigma Chemical, St. Louis, MO, USA), 1,2-distearoyl-*sn*-glycero-3-phosphoethanolamine-*N*-(PEG-2000) (PEG-DSPE), egg L-α-phosphatidylcholine (EPC), egg L-α-phosphatidylglycerol (EPG) or distearoyl phosphatidylcholine (DSPC) (Avanti Polar Lipids, Alabaster, AL, USA) were dissolved in chloroform:methanol in a round bottom flask. The solvent was evaporated under reduced pressure in a rotary evaporator and the lipid mixture was dried under nitrogen for 15 min, redissolved in 2-methyl-2-propanol (Sigma Chemical, St. Louis, MO, USA) and freeze-dried overnight. The dried lipids were hydrated for 2 h in *N*-(2-hydroxy ethyl) piperazine-*N*′-ethane sulfonic acid (HEPES)/NaCl buffer, pH 7.4 (10 mM HEPES) (Sigma Chemical, St. Louis, MO, USA) and 135 mM NaCl (Merck, Darmstadt, Germany) containing 5 mM of the chelator deferoxamine mesylate (Desferal) (Novartis, Basel, Switzerland). The chelator was added to enable labelling with ^{67}Ga (see Section 2.3).

Liposomes of approximately 100 nm (range 80–120 nm) were obtained by sonication of the hydrated lipid dispersion for 8 min with an amplitude of 8 μ using a 9.5 mm probe in a MSE Soniprep 150 (Sanyo Gallenkamp PLC, Leicester, UK). To study the effect of particle size, liposome populations of three different mean sizes (i.e. 100, 280 and 360 nm) were obtained by multiple extrusion of the hydrated lipid dispersion through two stacked polycarbonate membranes (Nuclepore, Pleasanton, CA, USA) with pore sizes of 100 and 100 nm for the 100 nm liposomes, 400 and 200 nm for the 280 nm liposomes and 600 and 400 nm for the 360 nm liposomes.

Particle size distribution was measured using dynamic light scattering, detected at an angle of 90° to the laser beam on a Malvern 4700 System (Malvern Instruments, Malvern, UK). The polydispersity of the liposome population is reported by the system as a value between zero and one. A reported value of one indicates large variations in particle size, whereas a value of zero indicates a complete monodisperse system. For all liposome preparations used in the experiments, the polydispersity index value was below 0.3.

The ζ-potential of 0, 5 or 30 mol% EPG containing liposomes was measured using a zetasizer equipped with PCS v1.35 software (Malvern Instruments, Malvern, UK). Liposomes were prepared in 5% aqueous HEPES/NaCl buffer and the instrument was calibrated with electrophoresis standard latex particles.

2.3. Liposome labelling

To remove non-encapsulated deferoxamine, liposomes were applied on a Sephadex G-50 column (Pharmacia, Uppsalla, Sweden) and eluted with HEPES/NaCl buffer followed by concentration via ultracentrifugation at 60 000 rpm for 2 h at 4°C in a Beckman ultracentrifuge L-70 (Beckman, Palo Alto, CA, USA). Liposomes were labelled with ^{67}Ga according to Gabizon et al. [19]. ^{67}Ga-citrate (1 mCi/ml) (Mallinckrodt Medical, Petten, The Netherlands) was diluted 1:10 in aqueous 5 mg/ml 8-hydroxyquinone (Sigma Chemical, St. Louis, MO, USA) and incubated for 1 h at 52°C to yield ^{67}Ga-oxine. 1 ml of this mixture was added per 1000 μmol total lipid (TL) of liposomes. Since ^{67}Ga-oxine can pass the liposomal membrane and has a high affinity for the encapsulated chelator deferoxamine, the radioactive label becomes entrapped. ^{67}Ga-deferoxamine is an appropriate label for monitoring intact liposomes in the circulation as it is encapsulated in the liposome interior and it is excreted rapidly via the kidneys in case it leaks from circulating liposomes [19]. Free label was removed by gel filtration. Radiolabelled liposomes were concentrated by ultracentrifugation at 60 000 rpm for 2 h at 4°C in a Beckman ultracentrifuge L-70 (Beckman, Palo Alto, CA, USA). Resulting specific activities were between 4×10^4 and 2×10^5 cpm/μmol TL. The phosphate concentration was determined colorimetrically according to Bartlett [20].

2.4. Blood volume and organ blood content

Total blood volume of the infected rats was 5.3% of the body weight. This percentage was determined by labeling syngeneic erythrocytes with ^{111}In-oxine according to Kurantsin-Mills [21]. Briefly, in an in-

dependent experiment, blood samples were taken at 10 min after injection of the labeled erythrocytes assuming that all erythrocytes were still present in the circulation. The dilution factor of the radioactive ^{111}In-label allowed calculation of the total blood volume as well as the blood content of the various organs.

2.5. Blood circulation kinetics and biodistribution

Experimental groups consisted of six rats. Liposomes were administered intravenous (i.v.) at the selected dose (indicated in the text) via the tail vein at 40 h after bacterial inoculation of the left lung. Blood samples of approximately 0.3 ml were taken from alternating groups of three rats by retro-orbital bleeding using heparinized capillaries at 1, 4, 8, 12 and 16 h after liposome injection. All rats were bled at 24 h after injection. The blood sample volume was measured and radioactivity was counted in a Minaxi autogamma 5000 gamma counter (Packard Instrument Company, Meriden, CT, USA) allowing for calculation of the radioactivity present in the blood (see Section 2.4).

At 24 h after injection, rats were killed by CO_2 inhalation and infected left lung, right lung, spleen, kidneys, liver and heart were dissected. The organs were weighed and radioactivity was counted to assess the biodistribution of the liposomes. The contribution of radioactivity in the blood to the radioactivity measured in the organs was subtracted (see Section 2.4).

2.6. Statistical analysis

Pharmacokinetic studies have shown that SSL exhibit single first-order clearance rates independent of the dose [9,22]. Similarly, in our experiments, the circulation kinetics of individual animals between 1 and 24 h after injection could be well-described by a linear relationship on a semi-logarithmic plot ($0.88 < r < 1.00$).

Data were tested for homogeneity of variance using Levene's test. In case of significant differences in variance between groups, data were log-transformed. The paired *t*-test was used to compare infected left lung and right lung localization. Comparisons between groups were made by one-way analysis of variance corrected for multiple comparisons by the Bonferroni method using SPSS for Windows software release 7.5.2 (Statistical Product and Service Solutions, Chicago, MI, USA).

3. Results

At 40 h after bacterial inoculation of the left lung, at the time of liposome injection, three zones could be clearly distinguished in the lobar pneumonia area in the left lung: the early infected, hemorrhagic and consolidated zone. Furthermore, limited variation was noted in severity of infection between animals. At 40 h after bacterial inoculation, the inoculum of log 6 bacteria had multiplied to log 9.77 ± 0.24, whereas the original lung weight of 0.36 ± 0.07 g had increased to 1.07 ± 0.19 g (mean ± S.D., $n = 9$).

3.1. Effect of PEG density

The circulation kinetics and the biodistribution pattern of liposomes containing three different levels of PEG-DSPE with an approximate molecular weight of PEG of 2000 (i.e. 1, 5 or 10 mol%) are shown in Fig. 1A,B, respectively.

The 1 mol% PEG liposomes disappeared from the

→

Fig. 1. Effect of PEG density on blood clearance and biodistribution of liposomes. ^{67}Ga-deferoxamine-labelled liposomes were injected i.v. at 40 h after bacterial inoculation of the left lung with 10^6 *K. pneumoniae* cells at a dose of 75 μmol TL/kg body weight. The lipid composition was PHEPC:Chol:PEG-DSPE 1.85:1:0.15 mol:mol for the 5 mol% PEG-DSPE containing liposome preparation (particle size 104 nm, range 91–115 nm, $n = 8$), 1.97:1:0.03 mol:mol for the 1 mol% PEG-DSPE preparation (particle size 107 nm, range 98–116 nm, $n = 2$) and 1.7:1:0.3 mol:mol for the 10 mol% PEG-DSPE preparation (particle size 98 nm, range 96–100 nm, $n = 2$). (A) Liposome concentration in nmol TL/ ml blood (left *Y*-axis) and % of injected dose remaining in the circulation (right *Y*-axis) at indicated time points after injection. Data were calculated from radioactivity recovered ($n = 3$, mean ± S.D.). (B) Biodistribution of liposomes expressed as nmol TL/organ (left *Y*-axis) and % of injected dose/organ (right *Y*-axis) at 24 h after injection. Data were calculated from radioactivity recovered ($n = 6$, mean ± S.D.). LL = infected left lung, RL = right lung, Spl = spleen, Li = liver. * = $P < 0.05$, ** = $P < 0.01$, *** = $P < 0.001$. Significant differences are noted against the 5 mol% PEG-DSPE containing preparation.

bloodstream faster as compared to the 5 and 10 mol% PEG liposomes ($P<0.01$) (Fig. 1A). An increase of the PEG content from 5 up to 10 mol% did not affect the circulation kinetics. The biodistribution data show that, for all three PEG liposome preparations, the localization in the infected left lung at 24 h after injection was approximately 3–4-fold higher than the corresponding localization in the uninfected right lung ($P<0.001$) (Fig. 1B). Yet, the degree of localization in the infected left lung of the 1 mol% PEG liposomes was somewhat lower ($\pm 20\%$) compared to the 5 mol% PEG liposomes ($P<0.05$), while the extent of localization of the 5 and 10 mol% PEG liposomes in the infected lung was similar. The hepatosplenic uptake of the 1 mol% PEG liposomes was significantly higher than the

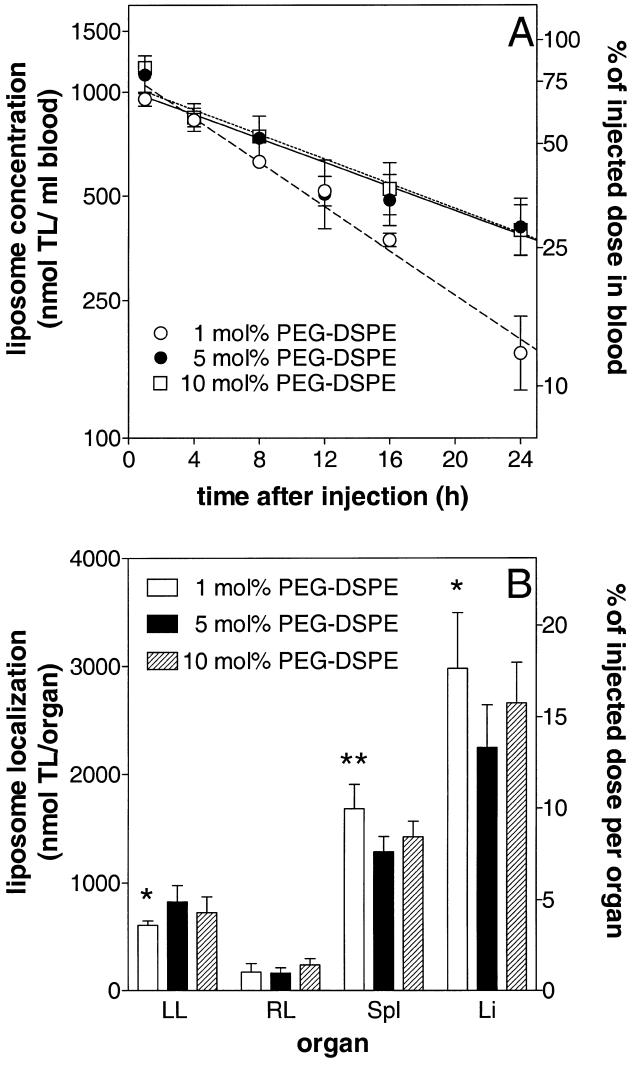

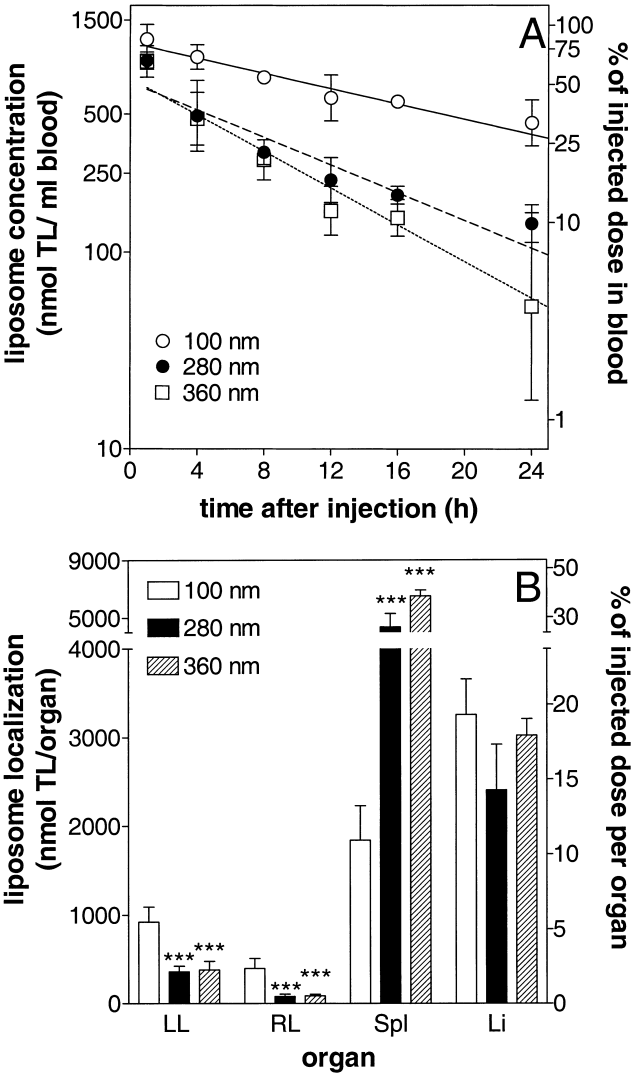

Fig. 2. Effect of particle size on blood clearance and biodistribution of liposomes. See Fig. 1 for details. The lipid composition of the liposomes was PHEPC:Chol:PEG-DSPE 1.85:1:0.15 mol:mol. 100 nm formulation particle size: 104 nm, range 91–115 nm, $n=8$; 280 nm formulation particle size: 277 nm, range 268–286 nm, $n=2$; 360 nm formulation particle size: 359 nm, range 331–387 nm, $n=2$. Significant differences against the 100 nm-sized liposome preparation are noted.

5 and 10 mol% PEG liposomes ($P<0.05$ and $P<0.005$, respectively). The latter two liposome types displayed a similar degree of localization in the liver and spleen. Localization in the uninfected right lung was not significantly different for the three different liposome preparations. Very low levels of liposome localization were seen in heart (<40

nmol TL) and kidneys (< 200 nmol TL) (data not shown).

3.2. Effect of particle size

The circulation kinetics and the biodistribution pattern of liposomes differing in mean size (i.e. 100, 280 and 360 nm) are shown in Fig. 2A,B, respectively. PEG liposomes with a mean size of 100 nm were removed from the bloodstream at a much lower rate as compared to the 280 and 360 nm liposome formulations ($P < 0.01$ and $P < 0.05$, respectively) (Fig. 2A). Regarding the biodistribution pattern, it was observed that the localization in the uninfected right lung and the infected left lung was approximately 2-fold lower in case of the 280 and 360 nm liposome preparations compared to the 100 nm PEG liposomes ($P < 0.001$) (Fig. 2B). Importantly, for each liposome formulation, the localization in the infected left lung was approximately 4-fold higher than in the uninfected right lung ($P < 0.001$). Splenic uptake appeared to increase considerably with an increasing size of the PEG liposomes ($P < 0.001$). The distribution to liver, heart (data not shown) and kidneys (data not shown) was not significantly different for any of the liposome preparations in this experiment.

3.3. Effect of bilayer fluidity

Bilayer fluidity is determined by the lipid composition of the liposome. Hydrogenated phospholipids yield rigid bilayers whereas more unsaturated phospholipids give bilayers a more fluid character [23]. Besides, Chol has also been shown to be an important modulator of bilayer fluidity by increasing bilayer rigidity and lateral packing [23]. The liposome preparations evaluated here vary, regarding bilayer fluidity, as follows (in order of increasing fluidity): DSPC:PEG-DSPE, PHEPC:PEG-DSPE, EPC:PEG-DSPE. One liposome preparation contains additionally Chol (i.e. PHEPC:Chol:PEG-DSPE) to examine the effect of inclusion of the steroid. The circulation kinetics and the biodistribution pattern of liposomes differing in bilayer fluidity are shown in Fig. 3A,B, respectively. The circulation times of all four liposome preparations evaluated were similar (Fig. 3A). Regarding the biodistribution profile, all four liposome formulations showed an approximately 4-fold higher localization in the infected left lung compared to the uninfected right lung ($P < 0.001$) (Fig. 3B). Tissue distribution patterns of the various liposome formulations were not significantly different.

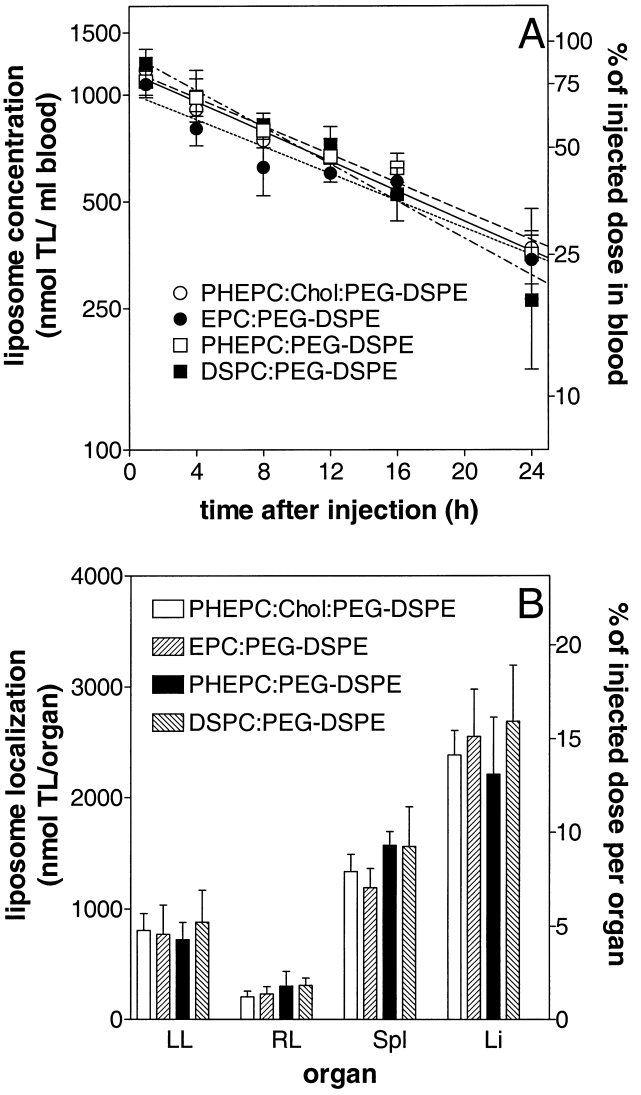

Fig. 3. Effect of bilayer fluidity on blood clearance and biodistribution of liposomes. See Fig. 1 for details. The lipid composition of the PHEPC:Chol:PEG-DSPE liposome was 1.85:1:0.15 mol:mol (particle size 104 nm, range 91–115 nm, $n = 8$), of the DSPC:PEG-DSPE 1.9:0.1 mol:mol (particle size 114 nm, range 95–133 nm, $n = 2$), of the PHEPC:PEG-DSPE 1.9:0.1 mol:mol (particle size 121 nm, range 109–133 nm, $n = 2$) and of the EPC:PEG-DSPE preparation 1.9:0.1 mol:mol (particle size 84 nm, range 76–92 nm, $n = 2$).

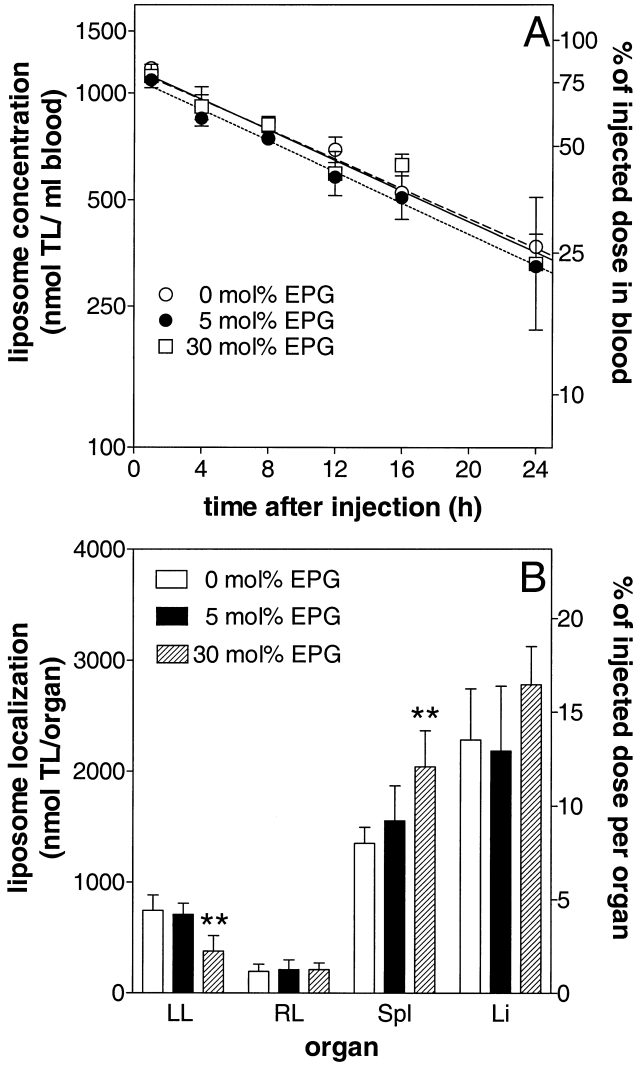

Fig. 4. Effect of the EPG level on blood clearance and biodistribution of liposomes. See Fig. 1 for details. The lipid composition was PHEPC:Chol:PEG-DSPE:EPG 1.85:1:0.15:0 mol:mol for the 0 mol% EPG containing liposome preparation (particle size 104 nm, range 91–115 nm, $n=8$), 1.7:1:0.15:0.15 mol:mol for the 5 mol % EPG preparation (particle size 93 nm, range 87–99 nm, $n=2$) and 0.95:1:0.15:0.9 mol:mol for the 30 mol% EPG preparation (particle size 82 nm, range 78–86 nm, $n=2$). Significant differences against the 0 mol% EPG containing liposome preparation are noted.

3.4. Effect of charged phospholipids

The circulation kinetics and the biodistribution pattern of PEG liposomes differing in EPG content (i.e. 0, 5 and 30 mol%) were determined to study the effect of charged phospholipids (Fig. 4A,B). The ζ-potentials of the 0, 5 and 30 mol% EPG containing liposomes were measured. The ζ-potential decreased slightly with an increasing EPG content, under the experimental conditions used, from -10.7 ± 1.1 mV for the 0 mol% EPG containing liposomes via -13.4 ± 1.4 mV for the 5 mol% EPG preparation to -19.7 ± 1.1 mV for the 30 mol% EPG containing liposomes (mean ± S.D., $n=3$ preparations).

Inclusion of the negatively charged phospholipid did not appear to influence the circulation characteristics of the PEG liposomes (Fig. 4A). The degree of localization in the infected lung was not affected by the inclusion of 5 mol% EPG. Remarkably, inclusion of 30 mol% EPG resulted in an approximately 2-fold reduced target localization compared to the PEG liposomes containing 0 and 5 mol% EPG ($P<0.01$) (Fig. 4B). But, for all three types of PEG liposomes differing in EPG content, the degree of localization in the infected left lung was higher than in the uninfected right lung ($P<0.01$). The 30 mol% EPG containing preparation showed a significantly increased splenic localization ($P<0.01$) compared to the 0 and 5 mol% EPG containing PEG liposomes. Distribution of the three PEG liposome types to liver, kidneys and heart was not significantly different (heart and kidney data not shown). Total accumulation within the infected left lung, right lung, liver and spleen was not significantly different between the liposome formulations differing in EPG content. (4572 ± 623, 4655 ± 855, 5406 ± 618 nmol TL/tissues for the 0, 5 and 30 mol% EPG containing liposomes, respectively, mean ± S.D., $n=6$).

4. Discussion

SSL, obtained by coating the liposome surface with PEG via inclusion of PEG-DSPE into the liposomes, display a considerably increased circulation time compared to conventional liposomes lacking the PEG coating [9,10,22,24]. This long-circulating property has been exploited to reach infectious sites localized outside the major MPS organs, the liver and spleen [14–17]. SSL-encapsulated gentamicin showed a superior therapeutic effect compared to the free drug in our rat model of acute unilateral pneumonia in the left lung caused by *K. pneumoniae* [13]. SSL are, therefore, attractive candidates for site-selective drug delivery of antimicrobial agents. In

order to be able to rationally optimize liposomal preparations for targeted drug delivery to non-MPS infectious foci, it is important to gain insight into the liposome characteristics potentially affecting the process of liposome localization at the infected site. In this study, the effects of PEG density, liposomal size, bilayer fluidity and charge on circulation kinetics and biodistribution of liposomes were evaluated in our rat pneumonia model.

Liposomes containing 1 mol% PEG displayed inferior localization at the infected site and a shorter circulation time compared to liposomes containing 5 or 10 mol% PEG. It has been shown previously in healthy animals that inclusion of 5–7.5 mol% PEG-DSPE is optimal for achieving maximal prolongation of the circulation time, in case of PEG with an approximate molecular weight of 2000 [24]. This finding is consistent with the present observations in a rat model of bacterial infection, showing a lack of effect of increasing the PEG density from 5 to 10 mol% on blood circulation time and tissue disposition (Fig. 1A,B). Inclusion of 1 mol% PEG-DSPE is, apparently, less efficient in prolonging the circulation time as compared to inclusion of 5 or 10 mol% PEG-DSPE. The lower localization in the infected left lung of the 1 mol% PEG-DSPE SSL is most likely related to the faster removal from the bloodstream, resulting in a reduced possibility to interact with the target site. However, it cannot be totally excluded that PEG has a direct effect as well. It has been shown in tumor bearing mice that PEG-coated liposomes have an intrinsically higher tumor vascular permeability coefficient than conventional liposomes [25]. In this view, the presence of 1 mol% PEG-DSPE may have resulted in a suboptimal PEG density to facilitate extravasation. Future experiments will focus on the relative importance of the circulation time versus the presence of a PEG coating.

A positive correlation between circulation times and infected lung localization is also apparent from the experiments on the effect of particle size on circulation kinetics and biodistribution of SSL. SSL with mean particle sizes of 280 or 360 nm show an approximately 2-fold lower target localization compared to the 100 nm PEG liposomes. Again, this may be related to differences in circulation times as 100 nm SSL are cleared more slowly from the bloodstream compared to the SSL with larger mean sizes. On the other hand, the reduced localization at the site of infection of the two liposome types with the larger mean size may also be a direct consequence of the particle size of the liposomes, which may have been too large to achieve equally efficient extravasation compared to the 100 nm PEG liposome preparation. Boerman and co-workers studied the effect of particle size of SSL on liposome localization in a focal infection in the calf muscle of rats. The studied particle sizes were between 90 and 220 nm. Their study showed that particle sizes, within this range, do not affect the degree of target localization [26]. On the basis of the present results, we speculate that a further increase of the particle size to sizes well above 220 nm is required to observe a significant reduction in localization at the site of infection. The higher splenic uptake of the larger PEG-coated liposomes, noticed in this study, has also been observed by Litzinger and colleagues for SSL of approximately 300 nm and was suggested to be due to a filtration effect within the splenic collagen fiber meshwork [27]. Although the infected lung localization of the two larger SSL is relatively low, it can nonetheless be argued that these liposomes are still attractive for the delivery of antimicrobials. The present results demonstrate that SSL with a mean particle size up to 360 nm are still able to localize preferentially in infected tissue, though less efficient in this regard than the 100 nm SSL. If the liposome-associated drug load is increased sufficiently for the larger liposomes, it can be envisaged that the net drug concentration at the target site may even be increased when larger SSL with suboptimal localization characteristics are used.

Since bilayer fluidity can be an important determinant of the release of liposome-encapsulated compounds, this liposome characteristic should also be considered regarding its effect on SSL localization at the site of infection. Generally, it is reported that release of encapsulated compounds increases with an increasing fluidity of the liposome bilayer, which has also been shown to affect the therapeutic efficacy [28–32]. Minimal variations were noticed in circulation kinetics and tissue distribution of the liposome formulations differing in bilayer fluidity. This finding is in agreement with previous results reported by Woodle et al. [10,33]. Apparently, bilayer fluidity of SSL may be chosen to optimize drug retention in the

blood stream and release profile at the site of infection without compromising target localization.

The only factor that appeared to adversely affect target site localization without compromising circulation kinetics was incorporation of 30 mol% EPG into the SSL formulation. Charged phospholipids are often added to a liposomal preparation to improve drug loading and/or stability of the formulation against aggregation during storage. The PEG coating has a distinct effect on the liposomal surface charge. The PEG coating moves the hydrodynamic plane of shear from the charged surface of the liposome to the edge of the PEG coating. The ζ-potential measurements as well as Gouy-Chapman calculations on the 0, 5 and 30 mol% EPG containing PEG liposomes suggested that in physiological ionic strength, the ζ-potential of the 30 mol% EPG SSL would be negligible at 2–3 nm from the surface, as the Debye length in this milieu is only 0.8 nm. Estimates for the thickness of the PEG coating, for PEG with a molecular weight of 2000, range from 3 to 5 nm [34,35]. Therefore, inclusion of EPG was not expected to have an effect on the circulation kinetics or biodistribution of SSL. However, the biodistribution profile of the 30 mol% EPG containing preparation shows an approximately 2-fold lower target localization compared to the 0 and 5 mol% EPG containing liposomes, but similar circulation kinetics as the 0 and 5 mol% EPG containing liposomes. It is speculated that the inclusion of 30 mol% EPG may have conferred a small but detectable negative ζ-potential at the edge of the PEG coating, allowing for interaction with biological components.

The results of the present study are to a certain degree in accordance with studies on pharmacokinetics and target localization of SSL in experimental tumor models. With respect to tumor localization of SSL, it is generally accepted that prolongation of the liposomal circulation time is beneficial for target localization [5,8–10,25,27,36]. The results regarding the effect of the PEG density, particle size and bilayer fluidity in the present study as well as previous results point in the same direction [12]. It has been demonstrated that tumor localization of SSL is a result of the increased microvascular permeability in malignant tissue [9,25]. As increased capillary permeability is also one of the hall marks of inflamed tissue, we suggest that selective SSL localization in infected tissue is a result of a similar effect of microvascular permeability changes.

In conclusion, SSL offer interesting possibilities for delivery of antibiotics to sites of bacterial infection localized outside the major MPS organs. It is shown here that the degree of localization at the infected site is remarkably independent of the physicochemical characteristics of the PEG liposomes. Substantial selective liposome localization can be achieved provided that certain criteria regarding PEG density, size and inclusion of charged phospholipids are met. In view of the differences in pharmacodynamics of the different classes of antibiotics, the rate and extent of release of encapsulated antibiotic from the PEG liposome extravasated into the infected site is an important issue. The present findings indicate that manipulation of the release profile by variation of the lipid composition may be possible without compromising the prolonged circulation and target localization properties. These properties seem to be a direct consequence of the presence of the polymer coating operating as a repulsive steric barrier opposing interactions with biological components.

Acknowledgements

This research was supported by Grant 902-21-161 of the Dutch Organization for Scientific Research (N.W.O.). Dr Zuidam is thanked for performing the Gouy-Chapman calculations.

References

[1] M. Venditti, P. Martino, The importance of in-vitro susceptibility testing in the management of compromised hosts, J. Chemother. 9S1 (1997) 116–122.
[2] J.D. Butts, Intracellular concentrations of antibacterial agents and related clinical implications, Clin. Pharmacokinet. 27 (1994) 63–84.
[3] R.H. Rubin, Fungal and bacterial infections in the immunocompromised host, Eur. J. Clin. Microbiol. Inf. Dis. 12S1 (1993) S42–48.
[4] K.M. Wasan, G. Lopez-Berestein, The past, present, and future uses of liposomes in treating infectious diseases, Immunopharmacol. Immunotoxicol. 17 (1995) 1–15.
[5] T.M. Allen, Liposomes opportunities in drug delivery, Drugs 54S4 (1997) 8–14.
[6] I.A.J.M. Bakker-Woudenberg, A.F. Lokerse, M.T. tenKate,

P.M. Melissen, W. vanVianen, E.W. vanEtten, Liposomes as carriers of antimicrobial agents or immunomodulatory agents in the treatment of infections, Eur. J. Clin. Microbiol. Infect. Dis. 12S1 (1993) S61–67.

[7] A.J. Schroit, J. Madsen, R. Nayar, Liposome-cell interactions: in vitro discrimination of uptake mechanism and in vivo targeting strategies to mononuclear phagocytes, Chem. Phys. Lipids 40 (1986) 373–393.

[8] G. Storm and M.C. Woodle, Long-circulating liposome therapeutics: from concept to clinical reality, in: M.C. Woodle and G. Storm (Eds.), Long Circulating Liposomes: Old Drugs, New Therapeutics. Springer-Verlag, Berlin, 1998, pp. 3–16.

[9] D. Papahadjopoulos, T.M. Allen, A. Gabizon, E. Mayhew, K. Matthay, S.K. Huang, K.-D. Lee, M.C. Woodle, D.D. Lasic, C. Redemann, F.J. Martin, Sterically stabilized liposomes: Improvements in pharmacokinetics and antitumor therapeutic efficacy, Proc. Natl. Acad. Sci. USA 88 (1991) 11460–11464.

[10] M.C. Woodle, M.S. Newman and P.K. Working, Biological properties of sterically stabilized liposomes, in: D.D. Lasic and F.J. Martin (Eds.), Stealth Liposomes. CRC Press, Boca Raton, FL, 1995, pp. 103–117.

[11] I.A.J.M. Bakker-Woudenberg, A.F. Lokerse, M.T. tenKate, G. Storm, Enhanced localization of liposomes with prolonged blood circulation time in infected lung tissue, Biochim. Biophys. Acta 1138 (1992) 318–326.

[12] I.A.J.M. Bakker-Woudenberg, A.F. Lokerse, M.T. tenKate, J.W. Mouton, M.C. Woodle, G. Storm, Liposomes with prolonged blood circulation and selective localization in *Klebsiella pneumoniae*-infected lung tissue, J. Infect. Dis. 168 (1993) 164–171.

[13] I.A.J.M. Bakker-Woudenberg, M.T. tenKate, L.E.T. Stearne-Cullen, M.C. Woodle, Efficacy of gentamicin or ceftazidime entrapped in liposomes with prolonged blood circulation and enhanced localization in *Klebsiella pneumoniae*-infected lung tissue, J. Infect. Dis. 171 (1995) 938–947.

[14] O.C. Boerman, W.J. Oyen, G. Storm, M.L. Corvo, L. vanBloois, J.W. vanderMeer, F.H. Corstens, Technetium-99m labeled liposomes to image experimental arthritis, Ann. Rheum. Dis. 56 (1997) 369–373.

[15] W.J. Oyen, O.C. Boerman, E.T. Dams, G. Storm, L. vanBloois, E.B. Koenders, U.J. vanHaelst, J.W. vanderMeer, F.H. Corstens, Scintigraphic evaluation of experimental colitis in rabbits, J. Nucl. Med. 38 (1997) 1596–1600.

[16] W.J. Oyen, O.C. Boerman, G. Storm, L. vanBloois, E.B. Koenders, R.A. Claessens, R.M. Perenboom, D.J.A. Crommelin, J.W. vanderMeer, F.H. Corstens, Detecting infection and inflammation with technetium-99m-labeled Stealth liposomes, J. Nucl. Med. 37 (1996) 1392–1397.

[17] V. Awasthi, B. Goins, R. Klipper, R. Loredo, D. Korvick, W.T. Phillips, Imaging experimental osteomyelitis using radiolabeled liposomes, J. Nucl. Med. 39 (1998) 1089–1094.

[18] I.A.J.M. Bakker-Woudenberg, J.C. vandenBerg, M.F. Michel, Therapeutic activities of cefazolin, cefotaxime, and ceftazidime against experimentally induced *Klebsiella pneumoniae* pneumonia in rats, Antimicrob. Agents Chemother. 22 (1982) 1042–1050.

[19] A. Gabizon, J. Huberty, R.M. Straubinger, D. Papahadjopoulos, An improved method for in vivo tracing and imaging of liposomes using a gallium 67-deferoxamine complex, J. Liposome Res. 1 (1988) 123–135.

[20] G.R.J. Bartlett, Phosphorus assay in column chromatography, J. Biol. Chem. 234 (1959) 466.

[21] J. Kurantsin-Mills, H.M. Jacobs, R. Siegel, M.M. Cassidy, L.S. Lessin, Indium-111 oxine labeled erythrocytes: cellular distribution and efflux kinetics of the label, Int. J. Rad. Appl. Instrum. B 16 (1989) 821–827.

[22] T.M. Allen, C. Hansen, Pharmacokinetics of stealth versus conventional liposomes: effect of dose, Biochim. Biophys. Acta 1068 (1991) 133–141.

[23] R.A. Demel, B. DeKruyff, The function of sterols in membranes, Biochim. Biophys. Acta 457 (1976) 109–132.

[24] T.M. Allen, C. Hansen, F. Martin, C. Redemann, A. Yau-Young, Liposomes containing synthetic lipid derivatives of poly(ethylene glycol) show prolonged circulation half-lives in vivo, Biochim. Biophys. Acta 1066 (1991) 29–36.

[25] M.W. Dewhirst and D. Needham, Extravasation of Stealth liposomes into tumors: direct measurement of localization and vascular permeability using a skin flap window chamber, in: D.D. Lasic and F.J. Martin (Eds.), Stealth Liposomes. CRC Press, Boca Raton, FL, 1995, pp. 127–137.

[26] O.C. Boerman, W.J. Oyen, L. vanBloois, E.B. Koenders, J.W. vanderMeer, F.H. Corstens, G. Storm, Optimization of technetium-99m-labeled PEG-liposomes to image focal infection: effects of particle size and circulation time, J. Nucl. Med. 38 (1997) 489–493.

[27] D.C. Litzinger, A.M. Buiting, N. vanRooijen, L. Huang, Effect of size on the circulation time and intraorgan distribution of amphiphatic poly(ethylene glycol)-containing liposomes, Biochim. Biophys. Acta 1190 (1994) 99–107.

[28] C. Beaulac, S. Clement-Major, J. Hawari, J. Lagace, Eradication of mucoid *Pseudomonas aeruginosa* with fluid liposome-encapsulated tobramycin in an animal model of chronic pulmonary infection, Antimicrob. Agents Chemother. 40 (1996) 665–669.

[29] I.A.J.M. Bakker-Woudenberg, A.F. Lokerse, F.H. Roerdink, Antibacterial activity of liposome-entrapped ampicillin in vitro and in vivo in relation to the lipid composition, J. Pharmacol. Exp. Ther. 251 (1989) 321–327.

[30] A. Nagayasu, T. Shimooka, H. Kiwada, Effect of vesicle size on in vivo release of daunorubicin from hydrogentaed egg phosphatidylcholine-based liposomes into blood circulation, Biol. Pharm. Bull. 18 (1995) 1020–1023.

[31] M. Silvander, M. Johnsson, K. Edwards, Effects of PEG-lipids on permeability of phosphatidylcholine/cholesterol liposomes in buffer and in human serum, Chem. Phys. Lipids 97 (1998) 15–26.

[32] C. Beaulac, S. Clement-Major, J. Hawari, J. Lagace, In vitro kinetics of drug release and pulmonary retention of microencapsulated antibiotic in liposomal formulations in relation

to the lipid composition, J. Microencapsul. 14 (1997) 335–348.
[33] M.C. Woodle, K.K. Matthay, M.S. Newman, J.E. Hidayat, L.R. Collins, C. Redemann, F.J. Martin, D. Papahadjopoulos, Versatility in lipid compositions showing prolonged circulation with sterically stabilized liposomes, Biochim. Biophys. Acta 1105 (1992) 193–200.
[34] M.C. Woodle, L.R. Collins, E. Sponsler, N. Kossovsky, D. Papahadjopoulos, F.J. Martin, Sterically stabilized liposomes. Reduction in electrophoretic mobility but not electrostatic surface potential, Biophys. J. 61 (1992) 902–910.
[35] R. Zeisig, K. Shimada, S. Hirota, D. Arndt, Effect of sterical stabilization on macrophage uptake in vitro and on thickness of the fixed aqueous layer of liposomes made from alkylphosphocholines, Biochim. Biophys. Acta 1285 (1996) 237–245.
[36] A.A. Gabizon, Liposome circulation time and tumor targeting: implications for cancer chemotherapy, Adv. Drug Del. Rev. 16 (1995) 285–294.